Effect of the repulsive core in the proton-neutron potential on deuteron elastic breakup cross sections

Yuen Sim Neoh,[1] Mengjiao Lyu,[1] Yoshiki Chazono,[1] and Kazuyuki Ogata[1,2,3,*]

[1]*Research Center for Nuclear Physics, Osaka University, Ibaraki 567-0047, Japan*

[2]*Department of Physics, Osaka City University, Osaka 558-8585, Japan*

[3]*Nambu Yoichiro Institute of Theoretical and Experimental Physics (NITEP), Osaka City University, Osaka 558-8585, Japan*

(Received 11 September 2019; accepted 30 April 2020; published 15 May 2020)

The role of the short-range part (repulsive core) of the proton-neutron (*pn*) potential in deuteron elastic breakup processes is investigated. A simplified one-range Gaussian potential and the Argonne V4′ (AV4′) central potential are adopted in the continuum-discretized coupled-channels (CDCC) method. The deuteron breakup cross sections calculated with these two potentials are compared. The repulsive core is found not to affect the deuteron breakup cross sections at energies from 40 MeV to 1 GeV. To understand this result, an analysis of the peripherality of the elastic breakup processes concerning the *pn* relative coordinate is performed. It is found that for the breakup processes populating the *pn* continua with orbital angular momentum ℓ different from 0, the reaction process is peripheral, whereas it is not for the breakup to the $\ell = 0$ continua (the *s*-wave breakup). The result of the peripherality analysis indicates that the whole spatial region of deuteron contributes to the *s*-wave breakup.

DOI: 10.1103/PhysRevC.101.054606

I. INTRODUCTION

The nucleon-nucleon (*NN*) interaction, the fundamental building block of nuclear physics, has been studied intensively using phase shift analysis [1,2], meson theory [3], chiral effective field theory [4,5], and lattice QCD [6]. It is well known that the *NN* interaction has a repulsive core at a short distance. It also contains many spin-dependent terms and, among them, the tensor part plays a crucial role in the binding mechanism of deuteron. Many efforts have been devoted to revealing roles of these characteristic features of the *NN* interaction in many-nucleon systems [7–14]. These have been studied also experimentally via electron- or proton-induced reactions [15–18]. In the same direction, breakup reactions of nuclei will be a possible way of probing the role of the short-range repulsion and tensor-induced attraction.

For many years, breakup reactions of weakly bound nuclei have been studied theoretically and experimentally. These studies are mainly motivated by interest in the natures of unstable nuclei and strong couplings with continuum states of fragile systems. The deuteron is the lightest weakly bound nucleus and its breakup processes have been measured since the early 1980s. The continuum-discretized coupled-channels method (CDCC) [19–21] is one of the most successful reaction models for describing the breakup processes of the deuteron and unstable nuclei. Its theoretical foundation was given in Refs. [22,23] and later numerically confirmed [24–26] via comparisons with Faddeev-Alt-Grassberger-Sandhas (FAGS) theory [27,28]. In most cases, a simplified one-range Gaussian potential [29] is employed for the *pn* interaction.

In this study, we consider the deuteron breakup as a possible probe for the above-mentioned striking features of the *pn* interaction. In Ref. [30], Iseri and collaborators compared CDCC results with the one-range Gaussian and Reid soft core [31] *pn* interactions for the cross section and polarization observables in deuteron elastic scattering. The difference is appreciable in tensor analyzing powers but not so significant except for a specific combination of polarization transfer coefficients. According to this finding, we focus on the central part of the *pn* interaction and use the Argonne V4′ (AV4′) [32] parametrization as a realistic *pn* interaction. It should be noted that the roles of the tensor and other spin-dependent terms in the Argonne V18 (AV18) interaction [33] are effectively included in the AV4′ interaction, that only has the central part. For simple notation, however, we regard the appearance of the short-range repulsive core as a characteristic of the AV4′ potential in what follows.

We investigate the effect of the short-range repulsive core on deuteron breakup cross sections at deuteron energies from 40 MeV to 1 GeV. Peripherality of the reaction process regarding the *pn* relative distance, which is crucial to understand whether the observable reflects the inner part of the *pn* wave function, is also investigated.

The organization of this paper is as follows. In Sec. II we summarize the method of CDCC, the results are discussed in Sec. III, and finally the conclusion is given in Sec. IV.

II. FORMALISM

We describe the deuteron breakup on a target nucleus *A* by a $p + n + A$ three-body model, assuming *A* to be inert.

*Corresponding author: kazuyuki@rcnp.osaka-u.ac.jp

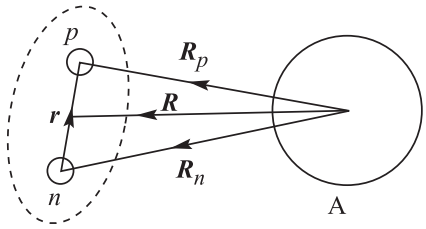

FIG. 1. Schematics of the three body system in deuteron scattering.

The coordinate labels are shown in Fig. 1. The three-body Hamiltonian is given by

$$H = T_{\boldsymbol{R}} + H_{pn} + V_{\rm CL}(R) + U_p(\boldsymbol{R}_p) + U_n(\boldsymbol{R}_n), \tag{1}$$

where T_X is the kinetic energy operator associated with the coordinate $\boldsymbol{X}$, $U_p(\boldsymbol{R}_p)$ and $U_n(\boldsymbol{R}_n)$ are the p-A and n-A distorting potentials, respectively, and $V_{\rm CL}(R)$ is the Coulomb potential between the center-of-mass (c.m.) of deuteron and A. The Hamiltonian H_{pn} of the pn system is given by

$$H_{pn} = T_{\boldsymbol{r}} + V_{pn}(\boldsymbol{r}), \tag{2}$$

where $V_{pn}(\boldsymbol{r})$ is the interaction potential between p and n. For the purpose of this investigation, only nuclear breakup is being considered and the intrinsic spin of the nucleon is disregarded.

In CDCC, the three-body wave function Ψ_{JM} with the total angular momentum J and its z component M is expanded in terms of the pn eigenstates $\hat{\phi}_{i\ell}$ consisting of the deuteron bound state and discretized continuum states of the pn system:

$$\Psi_{JM}(\boldsymbol{r},\boldsymbol{R}) = \sum_{i=0}^{i_{\max}} \sum_{\ell=0}^{\ell_{\max}} \sum_{L=|J-\ell|}^{J+\ell} \hat{\phi}_{i\ell}(r)\hat{\chi}_c^J(R)\mathcal{Y}_{\ell L}^{JM}, \tag{3}$$

$$\mathcal{Y}_{\ell L}^{JM} = [i^\ell Y_\ell(\hat{\boldsymbol{r}}) \otimes i^L Y_L(\hat{\boldsymbol{R}})]_{JM}, \tag{4}$$

where i and ℓ are the energy index and the orbital angular momentum of the pn system, respectively; $\hat{\phi}_{00}$ corresponds to the ground state of the deuteron. $\hat{\chi}_c^J$ describes the scattering motion of the c.m. of the pn system with respect to A, with L being the relative orbital angular momentum and $c = \{i, \ell, L\}$. The set $\{\hat{\phi}_{i\ell}\}$ satisfies

$$\int d\boldsymbol{r}\, \hat{\phi}^*_{i'\ell'}(r)Y^*_{\ell'm'}(\hat{\boldsymbol{r}})H_{pn}\hat{\phi}_{i\ell}(r)Y_{\ell m}(\hat{\boldsymbol{r}}) = \hat{\epsilon}_{i\ell}\delta_{i'i}\delta_{\ell'\ell}\delta_{m'm} \tag{5}$$

and is assumed to form a complete set in a space that is needed for describing a reaction process of interest.

If one inserts Eq. (3) into the Schrödinger equation

$$(H - E)\Psi_{JM}(\boldsymbol{r},\boldsymbol{R}) = 0 \tag{6}$$

and multiplies it by $\hat{\phi}^*_{i'\ell'}$ from the left, after the integration over $\boldsymbol{r}$, the following coupled-channels equations for $\hat{u}_c^J \equiv R\hat{\chi}_c^J$ are obtained:

$$\left(-\frac{\hbar^2}{2\mu_R}\nabla_R^2 + \frac{\hbar^2}{2\mu_R}\frac{L(L+1)}{R^2} + V_{\rm CL}(R) + \hat{\epsilon}_{i\ell} - E\right)\hat{u}_c^J(R) = -\sum_{c'} F_{cc'}(R)\hat{u}_{c'}^J(R), \tag{7}$$

where μ_R is the reduced mass of the deuteron-A system, E is the total energy, and the form factor $F_{cc'}$ is defined by

$$F_{cc'}(R) = \left\langle \hat{\phi}_{i\ell}(r)\mathcal{Y}_{\ell L}^{JM}\middle|U_p(\boldsymbol{R}_p) + U_n(\boldsymbol{R}_n)\middle|\hat{\phi}_{i'\ell'}(r)\mathcal{Y}_{\ell' L}^{JM}\right\rangle. \tag{8}$$

Here, the integration is understood to be done for $\boldsymbol{r}$ and $\hat{\boldsymbol{R}}$, and use has been made of Eq. (5).

Equations (7) are solved under the asymptotic boundary conditions of

$$\hat{u}_c(R) \to H^{(-)}_{\eta_i,L}(K_iR)\delta_{cc_0} - \sqrt{\frac{K_0}{K_i}}S_{cc_0}H^{(+)}_{\eta_i,L}(K_iR) \tag{9}$$

if $K_i = \sqrt{2\mu_R(E-\hat{\epsilon}_i)}/\hbar$ is real, and

$$\hat{u}_c(R) \to -S_{cc_0}W_{-\eta_i,L+1/2}(-2iK_iR) \tag{10}$$

if K_i is imaginary. Here, $H^{(+)}_{\eta_i,L}$ ($H^{(-)}_{\eta_i,L}$) is the outgoing (incoming) Coulomb wave function, $W_{-\eta_i,L+1/2}$ is the Whittaker function, and η_i is the Sommerfeld parameter. S_{cc_0} in Eq. (9) is the scattering matrix for the transition to channel c from the incident channel $c_0 = \{0, 0, J\}$. For more detail, readers are referred to Refs. [19–21].

III. RESULTS AND DISCUSSION

A. Model setting

We consider the deuteron scattering on a representative ^{58}Ni target at incident energies from 40 MeV to 1 GeV. At each energy, the nucleon-target distorting potential U_N ($N = p$ or n) is obtained by folding the Melbourne g-matrix interaction [34] with target density similar to the procedures described in Ref. [35]; below it is called the microscopic folding potential. We also use the EDAD1 parametrization of the Dirac phenomenology [36] for U_N to see the dependence of the result on the distorting potential. We assumed that in the Dirac phenomenology U_n is obtained in the same way as U_p but neglecting the Coulomb contribution. To investigate the role of the short-range repulsive core, we use two pn interactions. One is the AV4′ interaction and the other is the one-range Gaussian potential

$$V_{pn}(r) = -V_0 \exp\left(-\frac{r^2}{a^2}\right) \tag{11}$$

with $V_0 = 52.10$ MeV and $a = 1.812$ fm. The parameters are determined so that the binding energy (2.24 MeV) and the root-mean-square (rms) radius (2.01 fm) of the deuteron agree with the values obtained with the AV4′ interaction. In what follows, we denote this potential as 1G-av4. In Fig. 2(a), we show the AV4′ and 1G-av4 interactions by the solid and dashed lines, respectively. The corresponding wave functions of the deuteron ground state multiplied by r are shown in Fig. 2(b).

As for the CDCC model space, pn continua with $\ell = 0$, 2, and 4 are included, and $r_{\max} = R_{\max} = 60$ fm. At 80 MeV, the pn states are discretized with momentum bin size Δk of 0.05 fm^{-1} up to $k_{\max} = 1.5$ fm^{-1}, and $J_{\max} = 80$; at 1 GeV, $\Delta k = 0.25$ fm^{-1} and $k_{\max} = 3$ fm^{-1}, and $J_{\max} = 200$.

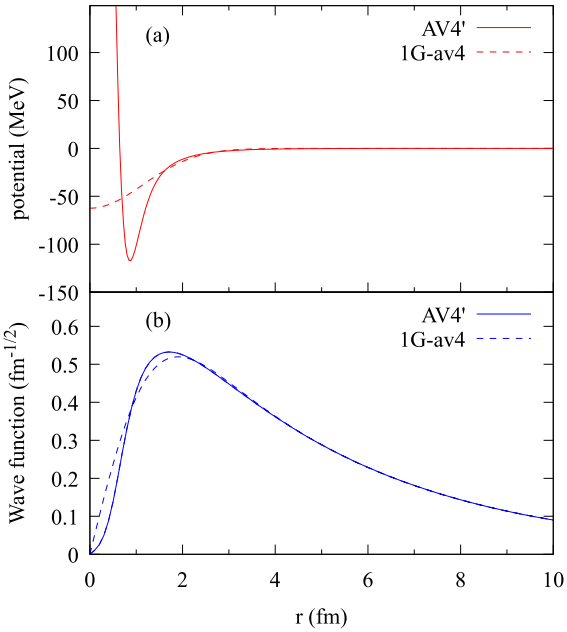

FIG. 2. (a) AV4′ (solid) and 1G-av4 (dashed) potentials. (b) Radial wave functions of deuteron multiplied by r.

B. Breakup cross section

Figure 3 shows the differential breakup cross sections at 80 MeV as a function of the pn relative momentum k calculated with the AV4′ (thick lines) and 1G-av4 (thin lines) potentials. As for U_N, the microscopic folding potential is used. The s-, d-, and g-wave components are shown by the dashed, dotted, and dash-dotted lines, respectively, and the solid lines are the sum of them. One sees that the difference between the AV4′ and 1G-av4 results for each partial-wave component is less than 2%.

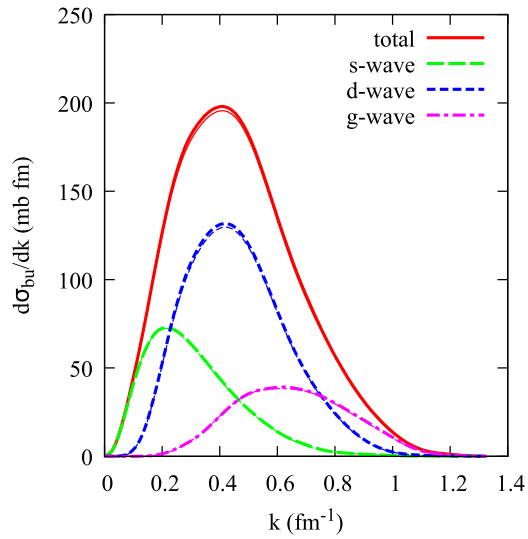

FIG. 3. Differential deuteron breakup cross sections on ^{58}Ni at 80 MeV as a function of the relative pn momentum (solid lines). The s-, d-, and g-wave components are shown by the dashed, dotted, and dash-dotted lines, respectively. The thick (thin) lines represent the results calculated with the AV4′ (1G-av4) potential. The microscopic folding potential is used as U_N.

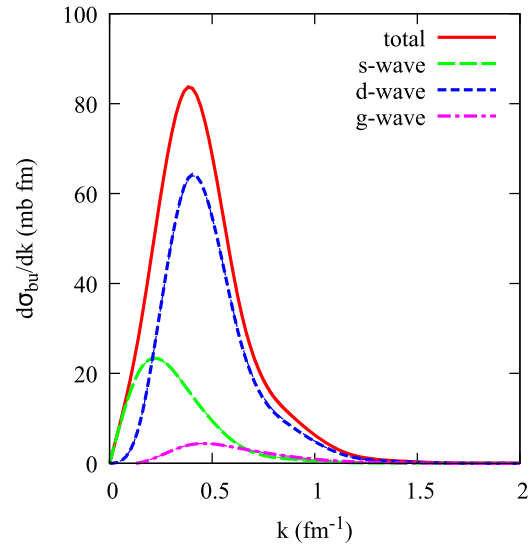

FIG. 4. Same as Fig. 3 but at 1 GeV.

One may expect that at higher incident energies we will have more chance to directly access the short-range part. However, as shown in Fig. 4, even at 1 GeV, the AV4′ and 1G-av4 potentials do not give an appreciable difference in the breakup cross sections. The integrated breakup cross sections as well as the breakdown into the partial-wave components are shown in Table I. The results obtained with the Dirac phenomenology for U_N are also shown. Although the values of $\sigma_{\rm bu}$ somewhat depend on U_N, the robustness of $\sigma_{\rm bu}$ against the change in V_{pn} is found for each U_N.

Thus, it is found that the short-range repulsive core of the AV4′ potential little affects the deuteron breakup cross sections on ^{58}Ni at 80 MeV and 1 GeV. We have confirmed the same feature also at 40 and 200 MeV (not shown). Furthermore, the negligible difference between the results with the two V_{pn} is found to be robust against the change in U_N.

C. Peripherality of deuteron breakup process

As seen from Fig. 2, the short-range repulsive core in the AV4′ potential modifies the inner region of the deuteron wave function. On the other hand, the breakup cross sections are found to be insensitive to the difference in V_{pn}. A possible indication of these findings is that the deuteron breakup process cannot probe the inner region of the deuteron, i.e., the reaction is peripheral with respect to the pn relative distance r.

To investigate the peripherality of the deuteron breakup, we follow the idea of the asymptotic normalization coefficient (ANC) method [37,38]. Even when the channel-couplings are taken into account, as in CDCC, the ANC can be deduced from an analysis of a peripheral reaction; for the details, readers are referred to Ref. [39]. We note here that our aim in this study is to investigate the peripherality of the deuteron breakup process and not to determine the value of the ANC of the pn system.

TABLE I. Total breakup cross section and its breakdown into partial-wave components for the deuteron on ^{58}Ni at 80 MeV and 1 GeV.

Energy	U_N	V_{pn}	Total (mb)	s-wave (mb)	d-wave (mb)	g-wave (mb)
80 MeV	microscopic	AV4′	106.7	27.3	58.4	21.0
		1G-av4	105.3	27.0	57.5	20.7
	Dirac	AV4′	136.8	35.3	73.2	28.2
		1G-av4	136.8	35.3	73.2	28.3
1 GeV	microscopic	AV4′	34.6	9.6	23.2	1.9
		1G-av4	34.7	9.6	23.2	1.9
	Dirac	AV4′	40.8	10.5	27.9	2.4
		1G-av4	40.9	10.6	27.9	2.4

In the asymptotic region, i.e., beyond the range r_N of V_{pn}, the deuteron wave function becomes

$$\varphi(r) \xrightarrow{r>r_N} b\exp(-\kappa r), \tag{12}$$

where $\kappa = (2\mu_{pn}\varepsilon/\hbar^2)^{1/2}$ with μ_{pn} being the pn reduced mass and ε the deuteron binding energy. b is the ANC if a realistic φ is used. In the present investigation, however, b is regarded to be just a constant. If the deuteron breakup is peripheral, the breakup cross section $\sigma_{\rm bu}$ is shown to be proportional to b^2 [39]. Then, if we change V_{pn}, b and $\sigma_{\rm bu}$ vary accordingly. Nevertheless, the proportionality factor

$$f \equiv \sigma_{\rm bu}/b^2 \tag{13}$$

does not change because of the peripherality. Therefore, f can be used as a measure of the peripherality.

We prepare six one-range Gaussian potentials which generate deuteron wave functions with rms radii ranging from 1.7 to 2.2 fm. Their depth and range parameters are shown in Table II. Figure 5 represents the resulting deuteron wave function divided by b; b is extracted at 6 fm.

Figure 6 shows f, normalized to the value at $r_{\rm rms} = 1.7$ fm, for each partial-wave component of the breakup cross section on ^{58}Ni at 80 MeV; the microscopic folding potential is adopted. For the d- and g-wave breakup, f is almost constant, which indicates the peripherality of the reaction. On the other hand, f for the s-wave breakup strongly depends on $r_{\rm rms}$. This means that the s-wave deuteron breakup is not peripheral. In Fig. 7 we show the result at 1 GeV. The general feature is the same as at 80 MeV but the $r_{\rm rms}$ dependence of the s-wave breakup is slightly weaker. It is found that this weakening is due to less importance of the multistep breakup processes at 1 GeV. In other words, at 80 MeV, multistep processes enhance the contribution from the inner part of the deuteron. The same trend is confirmed when we use the Dirac phenomenology for U_N.

Thus, the negligible difference between the breakup cross sections with the AV4′ and 1G-av4 interactions shown in Figs. 3 and 4 can be understood by the peripherality of the reaction, except for the s-wave breakup. On the other hand, the s-wave breakup is found to be not peripheral, which appears to contradict the finding shown in Figs. 3 and 4. A possible way of understanding the phenomenon will be that the whole spatial region of the deuteron is probed and the difference between the deuteron wave functions with the AV4′ and 1G-av4 interactions is smeared. As shown in Fig. 2, the solid line is larger than the dashed line between 1 and 2 fm, whereas the former is smaller than the latter at $r < 1$ fm. This may indicate that if a breakup process that selectively probes r larger than 1 fm was found, it could be a probe of the short-range repulsive core of V_{pn}.

TABLE II. One-range Gaussian potentials prepared for the peripherality study. Parameters of 1G-av4 are also listed. V_0 is determined to reproduce the binding energy calculated with the AV4′ potential.

Name	V_0 (MeV)	a (fm)	$r_{\rm rms}$ (fm)
1G-a	280.23	0.687	1.70
1G-b	131.42	1.047	1.80
1G-c	79.21	1.405	1.90
1G-d	54.35	1.765	2.00
1G-av4	52.10	1.812	2.01
1G-e	40.46	2.126	2.10
1G-f	31.76	2.492	2.20

IV. CONCLUSION

We have investigated the effect of the short-range repulsive core of the pn interaction on the deuteron breakup cross

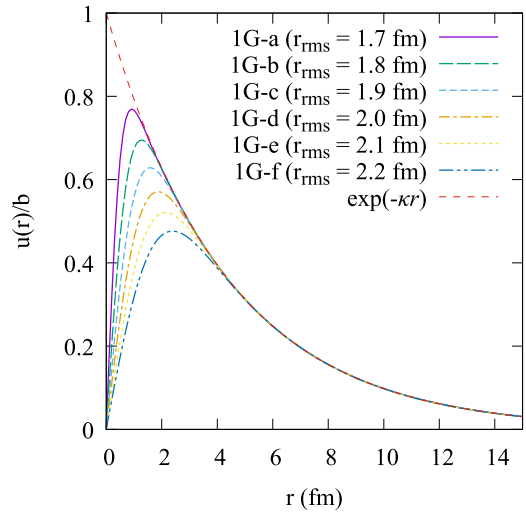

FIG. 5. Deuteron wave functions normalized to the exponential function at 6 fm.

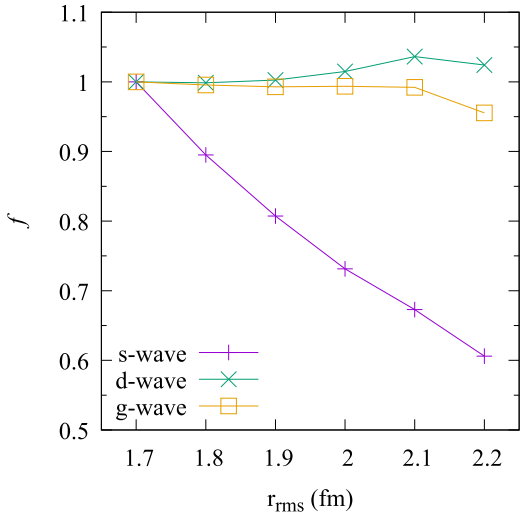

FIG. 6. f for each partial-wave component of the breakup cross section on ^{58}Ni at 80 MeV. The horizontal axis is the rms radii of the deuteron adopted. The values of f are normalized to the value at $r_{\rm rms} = 1.7$ fm. The microscopic folding potential is used as U_N.

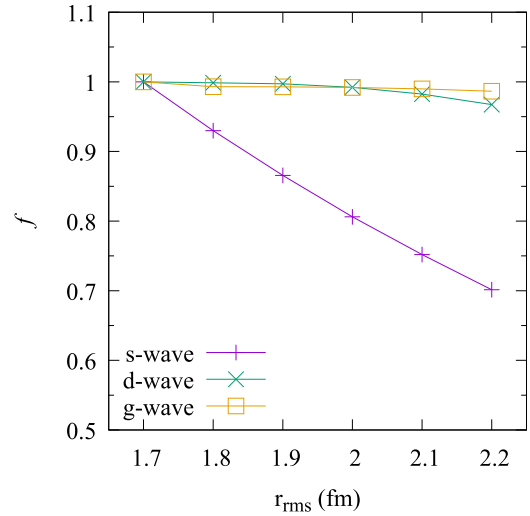

FIG. 7. Same as Fig. 6 but at 1 GeV.

sections on ^{58}Ni at incident energies from 40 MeV to 1 GeV. While the deuteron wave function is affected by the repulsive core at the pn distance r less than 2 fm, the deuteron breakup cross section changes very little. This insensitivity is found to be due to the peripherality of the reaction process concerning r except for the s-wave breakup. The s-wave breakup is found to be nonperipheral. The insensitivity of the s-wave breakup cross section to the short-range repulsive core may suggest that this reaction probes the whole spatial region of the deuteron. The exact extent and mechanism of the nonperipheral characteristic of the s-wave breakup will need further investigation.

ACKNOWLEDGMENTS

The authors would like to thank Shin Watanabe and Jagjit Singh for fruitful comments and discussions. This work was supported in part by Grants-in-Aid of the Japan Society for the Promotion of Science (Grant No. JP16K05352).

[1] R. A. Arndt, W. J. Briscoe, I. I. Strakovsky, and R. L. Workman, Phys. Rev. C **76**, 025209 (2007).
[2] R. L. Workman, W. J. Briscoe, and I. I. Strakovsky, Phys. Rev. C **94**, 065203 (2016).
[3] R. Machleidt, Phys. Rev. C **63**, 024001 (2001).
[4] E. Epelbaum, H.-W. Hammer, and Ulf-G. Meißner, Rev. Mod. Phys. **81**, 1773 (2009).
[5] R. Machleidt and D. Entem, Phys. Rep. **503**, 1 (2011).
[6] N. Ishii, S. Aoki, and T. Hatsuda, Phys. Rev. Lett. **99**, 022001 (2007).
[7] J. Carlson, S. Gandolfi, F. Pederiva, S. C. Pieper, R. Schiavilla, K. E. Schmidt, and R. B. Wiringa, Rev. Mod. Phys. **87**, 1067 (2015).
[8] G. Hagen, T. Papenbrock, M. Hjorth-Jensen, and D. J. Dean, Rep. Prog. Phys. **77**, 096302 (2014).
[9] B. R. Barrett, P. Navrátil, and J. P. Vary, Prog. Part. Nucl. Phys. **69**, 131 (2013).
[10] D. Lee, Prog. Part. Nucl. Phys. **63**, 117 (2009).
[11] R. Roth, T. Neff, and H. Feldmeier, Prog. Part. Nucl. Phys. **65**, 50 (2010).
[12] E. Hiyama, Prog. Theor. Exp. Phys. **2012**, 01A204 (2012).
[13] T. Myo, H. Toki, K. Ikeda, H. Horiuchi, and T. Suhara, Prog. Theor. Exp. Phys. **2015**, 073D02 (2015).
[14] M. Lyu, T. Myo, M. Isaka, H. Toki, K. Ikeda, H. Horiuchi, T. Suhara, and T. Yamada, Phys. Rev. C **98**, 064002 (2018).
[15] I. Korover *et al.* (Jefferson Lab Hall A Collaboration), Phys. Rev. Lett. **113**, 022501 (2014).
[16] O. Hen *et al.*, Science **346**, 614 (2014).
[17] M. Duer *et al.* (CLAS Collaboration), Nature (London) **560**, 617 (2018).
[18] S. Terashima, L. Yu, H. J. Ong, I. Tanihata, S. Adachi, N. Aoi, P. Y. Chan, H. Fujioka, M. Fukuda, H. Geissel, G. Gey, J. Golak, E. Haettner, C. Iwamoto, T. Kawabata, H. Kamada, X. Y. Le, H. Sakaguchi, A. Sakaue, C. Scheidenberger, R. Skibiński, B. H. Sun, A. Tamii, T. L. Tang, D. T. Tran, K. Topolnicki, T. F. Wang, Y. N. Watanabe, H. Weick, H. Witała, G. X. Zhang, and L. H. Zhu, Phys. Rev. Lett. **121**, 242501 (2018).
[19] M. Kamimura, M. Yahiro, Y. Iseri, Y. Sakuragi, H. Kameyama, and M. Kawai, Prog. Theor. Phys. Suppl. **89**, 1 (1986).
[20] N. Austern, Y. Iseri, M. Kamimura, M. Kawai, G. Rawitscher, and M. Yahiro, Phys. Rep. **154**, 125 (1987).
[21] M. Yahiro, K. Ogata, T. Matsumoto, and K. Minomo, Prog. Theor. Exp. Phys. **2012**, 01A206 (2012).
[22] N. Austern, M. Yahiro, and M. Kawai, Phys. Rev. Lett. **63**, 2649 (1989).
[23] N. Austern, M. Kawai, and M. Yahiro, Phys. Rev. C **53**, 314 (1996).
[24] A. Deltuva, A. M. Moro, E. Cravo, F. M. Nunes, and A. C. Fonseca, Phys. Rev. C **76**, 064602 (2007).
[25] N. J. Upadhyay, A. Deltuva, and F. M. Nunes, Phys. Rev. C **85**, 054621 (2012).

[26] K. Ogata and K. Yoshida, Phys. Rev. C **94**, 051603(R) (2016).
[27] L. D. Faddeev, Zh. Eksp. Theor. Fiz. **39**, 1459 (1960) [Sov. Phys. JETP **12**, 1014 (1961)].
[28] E. Alt, P. Grassberger, and W. Sandhas, Nucl. Phys. B **2**, 167 (1967).
[29] T. Ohmura, B. Imanishi, M. Ichimura, and M. Kawai, Prog. Theor. Phys. **43**, 347 (1970).
[30] Y. Iseri, M. Tanifuji, H. Kameyama, M. Kamimura, and M. Yahiro, Nucl. Phys. A **533**, 574 (1991).
[31] R. V. Reid, Ann. Phys. (NY) **50**, 411 (1968).
[32] R. B. Wiringa and S. C. Pieper, Phys. Rev. Lett. **89**, 182501 (2002).
[33] R. B. Wiringa, V. G. J. Stoks, and R. Schiavilla, Phys. Rev. C **51**, 38 (1995).
[34] K. Amos, P. J. Dortmans, H. V. von Geramb, S. Karataglidis, and J. Raynnal, in *Advances in Nuclear Physics*, edited by J. W. Negele and E. Vogt (Springer, New York, 2000), pp. 275–536.
[35] Y. S. Neoh, K. Yoshida, K. Minomo, and K. Ogata, Phys. Rev. C **94**, 044619 (2016).
[36] E. D. Cooper, S. Hama, B. C. Clark, and R. L. Mercer, Phys. Rev. C **47**, 297 (1993).
[37] A. M. Mukhamedzhanov and N. K. Timofeyuk, JETP Lett. **51**, 282 (1990).
[38] H. M. Xu, C. A. Gagliardi, R. E. Tribble, A. M. Mukhamedzhanov, and N. K. Timofeyuk, Phys. Rev. Lett. **73**, 2027 (1994).
[39] K. Ogata, S. Hashimoto, Y. Iseri, M. Kamimura, and M. Yahiro, Phys. Rev. C **73**, 024605 (2006).